

Evolution of collectivity in ^{118}Xe

C. Müller-Gatermann^{1,2,*}, A. Dewald², C. Fransen², M. Beckers², A. Blazhev², T. Braunroth²,
A. Goldkuhle², J. Jolie², L. Kornweibel², W. Reviol¹, F. von Spee², and K. O. Zell²

¹Physics Division, Argonne National Laboratory, 9700 South Cass Avenue, Lemont, Illinois 60439, USA

²Institut für Kernphysik der Universität zu Köln, Zùlpicher Str. 77, D-50937 Köln, Germany



(Received 27 May 2020; accepted 7 December 2020; published 21 December 2020)

A recoil-distance Doppler shift experiment has been performed using the $^{102}\text{Pd}(^{19}\text{F}, p2n)$ reaction at a beam energy of 73 MeV to measure the lifetime of excited states in ^{118}Xe . The differential decay-curve method using $\gamma\gamma$ coincidences and a gating procedure that allows to extract the lifetime without feeding assumptions has been employed. The lifetimes obtained for the yrast states up to spin-parity 8^+ are compared with interacting boson model calculations and ^{118}Xe can be classified as a transitional nucleus between the spherical and a deformed shape. Systematics of the $B(E2)$ values for the $2^+ \rightarrow 0^+$ and $4^+ \rightarrow 2^+$ transitions in the isotopic chains of tin, tellurium and xenon are presented. It is proposed that a “critical point” exists at which the $B(E2; 4^+ \rightarrow 2^+)/B(E2; 2^+ \rightarrow 0^+)$ ratio drops to unity for lower neutron numbers within the isotopic chain. The position of the “critical point” varies with proton number, i.e., it is presumed to be located at the same mass number $A = 114$ in the Sn, Te, and Xe isotopes.

DOI: [10.1103/PhysRevC.102.064318](https://doi.org/10.1103/PhysRevC.102.064318)

I. INTRODUCTION

The reduced transition probabilities of proton-rich nuclei northeast of ^{100}Sn show two interesting trends, which are not fully understood. For an isotopic (isotonic) chain of even-even nuclei the $B(E2; 2^+ \rightarrow 0^+)$ value is expected to increase in first order linearly towards neutron (proton) midshell. Casten introduced a so-called $N_\pi N_\nu$ scheme that in many cases correlates the increase in $B(E2)$ with the number of valence proton N_π (valence neutrons N_ν) remarkably well [1]. This correlation is also true for the Sn isotopes between neutron number $N = 70$ and the $N = 82$ shell gap as well as for the chain of the neighboring even-even nuclides of tellurium. For the lighter Sn isotopes, close to neutron midshell ($N = 66$) contradictory data exist showing a saturation or even a dip in the trend of the transition strengths. Below neutron midshell and until ^{104}Sn is reached the $B(E2)$ value as a function of N remains to be near constant, i.e., it does not mirror the down slope on the more neutron-rich side. The data on tellurium isotopes below neutron midshell show a similar behavior. The second observation is that the $B_{4/2} = B(E2; 4^+ \rightarrow 2^+)/B(E2; 2^+ \rightarrow 0^+)$ ratio is close to or even below unity for Sn and Te nuclei below neutron midshell, again in contrast to the above-midshell behavior. In the former case, a significant drop in $B(E2; 4^+ \rightarrow 2^+)$ values causes the decrease of the $B_{4/2}$ ratio. A summary of transition strengths in even Sn and Te isotopes is given in Fig. 1.

Seniority is a good quantum number for magic nuclei and together with shell effects it could give an explanation of these trends, which remain puzzling though. Indeed the authors

of Ref. [2] have proposed an explanation for $B_{4/2} \leq 1$ in a chain of semimagic nuclei based on an opposite behavior for $B(E2; 2^+ \rightarrow 0^+)$ and $B(E2; 4^+ \rightarrow 2^+)$ values near midshell. Recently, Togashi *et al.* [3] and Siciliano *et al.* [4] published different interpretations of the Sn isotopes both based on the shell model. Hitherto, the experimental data especially for higher lying states or/and for neighboring nuclei with $Z \geq 50$ are scarce. As for the latter aspect, there seems to be a strong demand for new data—in these nuclei with a more collective behavior the systematic trend of $B(E2; 4^+ \rightarrow 2^+)$ strengths below neutron midshell is unclear. In this work it is examined if the above effects in the Sn isotopic chain extend also to the even xenon isotopes. As a starting point ^{118}Xe is chosen, where the reduction of transition strength seems to be shifted to the 6^+ state [5]. Older experimental data [6,7] would be also consistent with a $B_{4/2}$ ratio around unity. All of these experiments were recoil-distance Doppler shift (RDDS) measurements employing γ -ray singles with feeding assumptions. The present analysis employed the differential decay-curve method (DDCM) [8] with gates on feeding transitions circumventing the feeding problem. So far $\gamma\gamma$ -coincidence data existed for the xenon isotopes with $A \geq 120$ and ^{114}Xe enabling an analysis without assumptions. The main goal of the present study is to clarify the spin-dependent evolution of transition strengths in ^{118}Xe . Since the nucleus is an isotone of the critical point nucleus ^{114}Sn [9], the properties of the former provide an additional test for IBM-type calculations [10].

II. EXPERIMENTAL DETAILS

Excited states of ^{118}Xe were populated in a heavy-ion induced fusion-evaporation reaction at the FN tandem

*cmuellergatermann@anl.gov

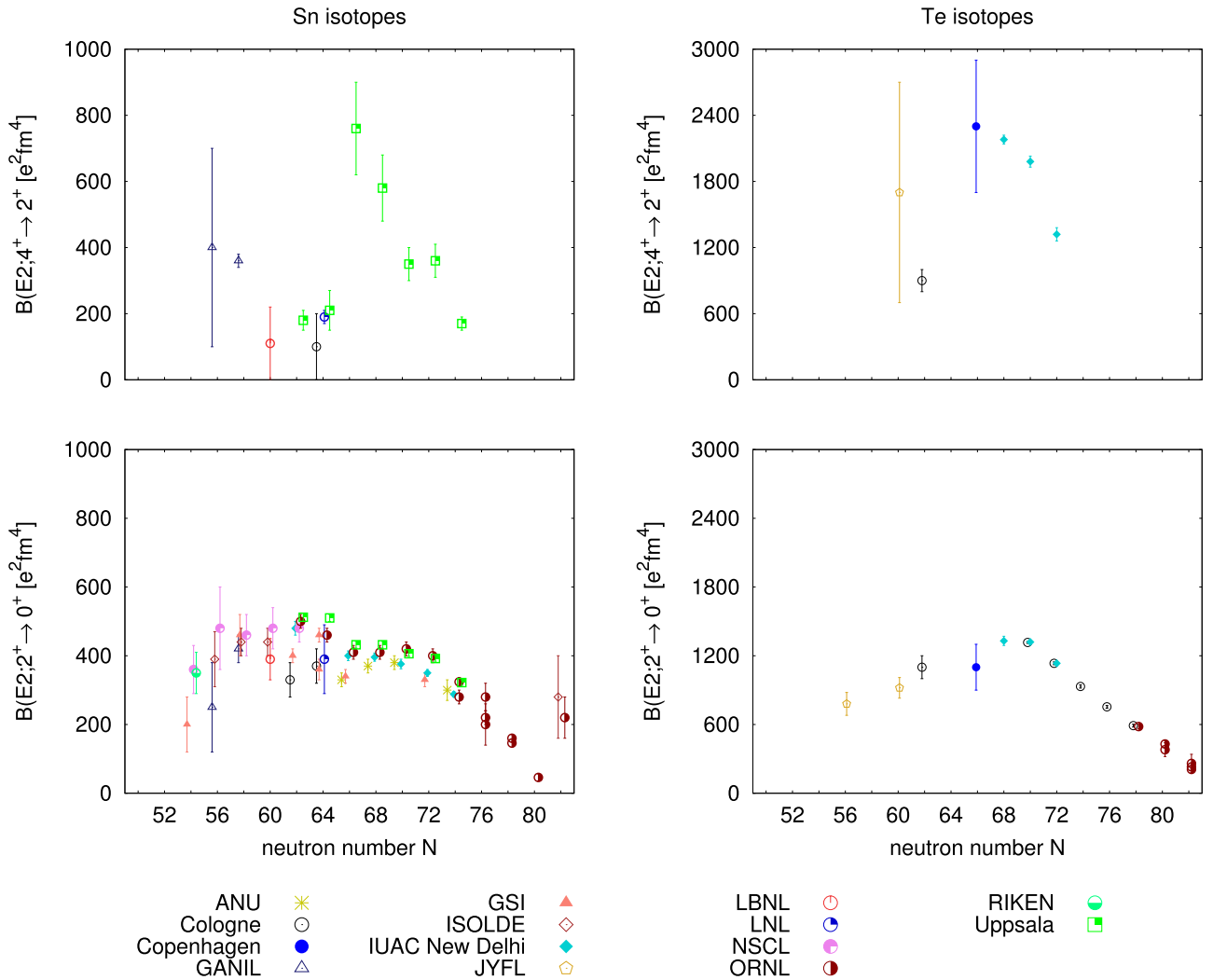


FIG. 1. Evolution of $B(E2; 2^+ \rightarrow 0^+)$ and $B(E2; 4^+ \rightarrow 2^+)$ values for the even tin and tellurium isotopes between the shell closures at $N = 50$ and $N = 82$. Different records for the same neutron number have been shifted slightly horizontally to sustain readability. The legend for all panels is given below, symbols are assigned to the facilities where the data was recorded. Note the different scale for the chains of isotopes. Evidently, the Sn isotopes exhibit an excess of transition strength for the $2^+ \rightarrow 0^+$ transition and a drop for the $4^+ \rightarrow 2^+$ transition below neutron midshell. Experimental data taken from [4,9,11–28] and [29–39]. See text for details.

accelerator of the University of Cologne, where lifetimes of excited states were measured with the Cologne Coincidence Plunger [40]. The reaction $^{102}\text{Pd}(^{19}\text{F}, p2n)^{118}\text{Xe}$ at a beam energy of 73 MeV provided an average recoil velocity of $v/c = 1.091(14)\%$, with a target of 1.0 mg/cm² thickness and 69% enrichment. The typical beam current was 1–2 pA, limited by heating of the stretched plunger target and stopper foils and the maximum counting rate of 18 kHz per high-purity germanium (HPGe) detector. The HPGe-detector array consisted of eleven single crystals with relative efficiencies of 55–100% arranged in two rings at 45° (five detectors) and 142.3° (six detectors) with respect to the beam direction. The plunger device was installed housing the moving target as well as a 3.7 mg/cm² Au stopper foil in the focal point of the detectors and parallel to the target. The stopper foil thickness ensured to stop all recoiling fusion-evaporation residues. Two ^{22}Na sources were attached to the plunger chamber introducing around 300 Hz count rate per detector. The decays were

used for shift tracking of the whole data acquisition system (DAQ) together with the Coulomb-excitation lines of ^{197}Au . A ^{226}Ra source at the stopper-foil position was used for energy and efficiency calibration, but only the former was used in the analysis. As a digital DAQ five 80 MHz XIA DGF-4C Rev. F modules were used in a triggerless mode to record also the low-multiplicity events from the sources and from Coulomb excitation. Within about 100 h 15 different relative target-to-stopper distances were measured ranging from electrical contact to 500 μm . The data were sorted ringwise in $\gamma\gamma$ -coincidence matrices with a binning of 0.5 keV/channel after applying a random-background subtraction and requiring a prompt-coincidence window of 125 ns.

III. LIFETIME ANALYSIS

The lifetime analysis was performed applying the DDCM [8] with gates on Doppler-shifted components of direct

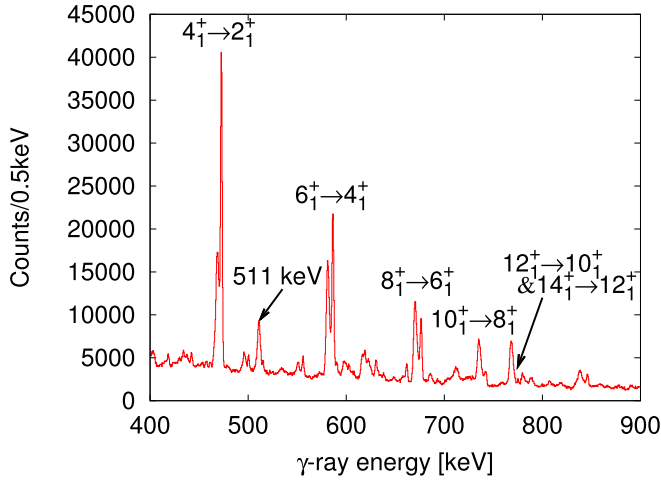


FIG. 2. Spectrum of the detectors in the ring at backward angles gated by the $2^+ \rightarrow 0^+$ transition for all distances. Marked are the yrast transitions up to the 14^+ state and the line from electron-positron annihilation. The unshifted and shifted (lower energy) peaks are clearly visible up to the $8^+ \rightarrow 6^+$ transition, and these initial states are analysed. See text for details.

feeding transitions only. This approach requires only relative target-to-stopper distances and eliminates any feeding contribution to the lifetime. Care was taken that the gates are clean, i.e., did not contain other transitions in the same nucleus or contaminant lines with similar energy. In the simplest case of a gate on the shifted (flight) component of a direct feeder the lifetime is calculated with the formula

$$\tau(x) = \frac{I_u(x)}{v \frac{d}{dx} I_s(x)}. \quad (1)$$

Here, I_u (I_s) is the normalized intensity of the unshifted (shifted) component of the depopulating transition, v is the recoil velocity, τ is the lifetime of the state, and x is the nominal target-to-stopper distance. The multiplication of v serves as a transformation that (relative) distances can be used instead of time of flight. Absolute distances are not needed in the analysis, the lifetime can be calculated for any distance x and should be independent of x . The relative distance is needed to calculate the derivative of the shifted component. A normalization of the γ -ray intensities for the different distances is done to compensate, e.g., for the different measuring times per distance and the beam current. In the best case the number of reactions of interest is used for the normalization, like it was done in this analysis. The derivation of formula (1) for γ -ray coincidences can be found in Ref. [8].

Figure 2 shows a summed spectrum over all distances measured with the backward-ring detectors and gated on the $2^+ \rightarrow 0^+$ transition. The yrast transitions in ^{118}Xe are clearly seen up to the 14^+ state and are marked in the figure. The 16^+ state is hardly visible in the summed spectrum and not in the spectra at individual distances. The decays of the 14^+ and 12^+ states form a doublet at 775 keV but only shifted components are visible in the spectra. Although a small unshifted component seems to be there for the $10^+ \rightarrow 8^+$ transition in the summed spectrum, it is not visible in the spectra for

TABLE I. Lifetimes and $B(E2)$ values of the lowest yrast states in ^{118}Xe . Column 3 contains individual lifetimes for each ring-ring combination, in column 4 the mean value is given, and column 5 indicates the literature values. γ -ray energies taken from [41].

I_i^π	E_γ [keV]	τ_i [ps]	$\bar{\tau}$ [ps]	$\tau_{\text{Lit.}}$ [ps]	$B(E2)$ [W.u.]
2_1^+	337.5	67.6(7)	68.6(10)		76.8(+11)
		69.6(7)			
4_1^+	472.8	7.9(2)	8.46(17)	65(4) [5]	$81(+5)$
		8.3(2)		65(3) [6]	$81(+4)$
		8.51(14)		69(5) [7]	$76(+5)$
		8.75(14)			$118(+2)$
				7.8(3) [5]	$127(+5)$
6_1^+	586.4	2.06(14)	2.18(9)	11(2) [6]	$90(+20)$
		2.1(2)			$58(+17)$
		2.4(2)		17(4) [7]	$156(+7)$
		2.5(3)			
				4.0(4) [5]	$85(+9)$
8_1^+	676.4	0.8(3)	1.17(13)	4.6(12) [6]	$70(+30)$
		0.9(8)		< 5 [7]	> 70
		1.0(6)			$143(+17)$
		1.0(3)			
		1.2(3)			
		1.3(3)			
		1.4(4)			
		1.8(4)			
			3.7(5) [5]	$44(+6)$	
			4.0(15) [6]	$42(+25)$	

one distance and a gate from above. This can be related to delayed feeding, which is not excluded with the gate from below in Fig. 2. The other, minor lines are also identified and are consistent with the recent level schemes of ^{118}Xe [41]. For example the line at 846 keV belongs to the $9^- \rightarrow 8^+$ decay. These decays were not strong enough for an unambiguous lifetime analysis especially if one wants to keep the gate from above. The present lifetime analysis is restricted to the lowest yrast states up to the 8^+ level. Earlier lifetime analyses [5–7] were vulnerable to systematic errors mainly due to unknown feeding. This is circumvented by the gate from above which is, within a reasonable amount of time, only possible nowadays with high efficiency setups and methods.

The lifetime analysis results are summarized in Table I. The lifetimes are a weighted mean of lifetimes corresponding to the four possible ring-ring combinations, except for the 2^+ state where only a gate in forward detectors was possible. Figure 3 presents a sample analysis, for the 4^+ state, which is performed with the computer code NAPATAU [42]. The top graph shows the lifetime extracted with Eq. (1) for each distance in the sensitive region. The sensitive region is

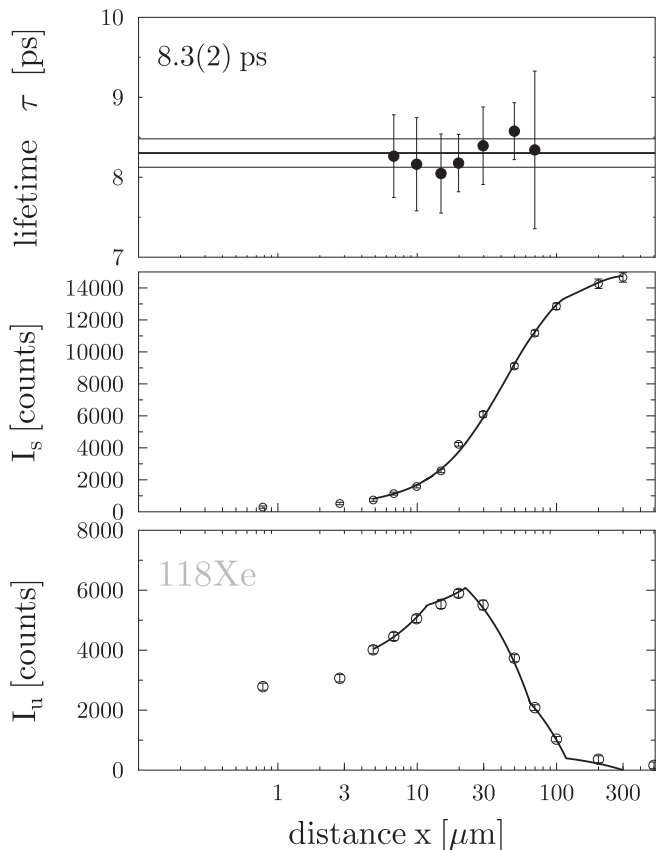


FIG. 3. Determination of the 4^+ -state lifetime analyzed with the detectors at backward angles using a gate on the shifted component of the $6^+ \rightarrow 4^+$ transition at forward angles. Top panel: Data points are the subset of τ values in the sensitive region, lower and upper horizontal lines represent the $\chi^2 + 1$ values and respective errors. Middle and bottom panels: Normalized shifted I_s and unshifted I_u intensities, respectively, and corresponding fitted functions. See text for details.

defined as the set of distances where the derivative of the shifted component is larger than half of the maximum slope. This is equivalent to the region where the unshifted component is larger than half of the maximum [see Eq. (1) with proportionality $v\tau$]. The middle graph shows the normalized intensities of the shifted component together with a best fit of second order polynomials. The bottom graph shows the corresponding unshifted component and the resulting curve for the lifetime. A common χ^2 minimization is employed for the polynomials with the shifted and the unshifted intensities. The $(\chi^2 + 1)$ limits can be seen as horizontal lines in the top panel and are given as the error. No systematic deviation from a constant trend can be seen for the individual τ values from the mean lifetime with the minimum χ^2 value. For the 2^+ state no gate could be applied for the backward detectors, because there was a ^{117}I contamination from the $2p2n$ side channel. The $(\frac{19}{2})^-$ state at 1485.2 keV in ^{117}I decays to the $(\frac{15}{2}^-)$ state at 1015.1 keV. The latter state decays via a 337.5 keV γ ray forming a doublet with the $2^+ \rightarrow 0^+$ transition in ^{118}Xe . The feeding

transition in ^{117}I of 470.1 keV overlaps with the shifted component of the $4^+ \rightarrow 2^+$ transition at backward angles (shift to lower energies). Ignoring this contamination reproduced the 2^+ lifetime of Refs. [5,6], although this could be just by chance. Below the shifted part of the 586.4 γ ray another contamination was found in both detector rings. It showed up as a “self-coincidence” to a long-lived state. It cannot originate from ^{118}Xe since only an unshifted component was visible and that combination is only possible if the lower state is long lived. The 6^+ state has no long lifetime and a state below would have been seen in the Gammasphere experiment of Ref. [41]. If the state was at higher excitation energies only a shifted component would be visible in the spectrum, because the decay would have to happen before. Although the γ ray was clearly seen and comparable to the $9^- \rightarrow 7^-$ transition in ^{118}Xe (10% relative intensity to $2^+ \rightarrow 0^+$ in Ref. [41]) it could not be identified via coincident γ rays. The highest yrast state for which shifted and unshifted components were visible with a gate on a shifted feeding transition was the 8^+ state. Here, two direct gates have been set on the $10^+ \rightarrow 8^+$ and the $9^- \rightarrow 8^+$ transition. The deceleration time in the stopper might be of the same order of magnitude as the lifetime for this decay. Therefore Doppler-shift attenuation (DSA) effects could possibly influence the line shape and would have to be corrected. As no such effects have been observed, no correction was applied. Using fixed calculated widths and positions for the two peaks (only peak areas as free parameter) the data were reproduced and no deviation between the fit and the spectra was found. The lineshape of the two peaks can be reproduced with two gaussian functions. In Ref. [43] the DSA effect is investigated in detail and a correction applied to a comparable experimental dataset. The correction amounts approximately the error given for the lifetime in this work. The difference to the present work is the stopping range in the gold stopper, which is a factor of 3.5 larger in Ref. [43] and the peaks shown therein differ from a gaussian shape. Figure 4 shows a typical spectrum for this transition using forward-angle detectors. The spectrum corresponds to the sum of distances with an unshifted component and the gate used is the shifted component of the feeding 10^+ state. Regarding the 8^+ state the impact of the DSA effect seems to be below the limit of sensitivity in the present dataset. No such effect would affect the extracted lifetime noticeably for the states with a longer lifetime.

IV. DISCUSSION

First of all it should be pointed out, that a reduction of the $B(E2; 6^+ \rightarrow 4^+)$ and $B(E2; 8^+ \rightarrow 6^+)$ values to the level of the $B(E2; 2^+ \rightarrow 0^+)$ value, as reported in Refs. [5–7] is not confirmed in the present work. That reduction seems to be related to delayed feeding, which could have biased the previous results. Second, the present $B_{4/2}$ ratio of 1.55 is not as close to unity as those in neighboring proton-rich Sn and Te isotopes. Third, the low $B(E2; 6^+ \rightarrow 4^+)$ value in previous work was attributed to a possible band crossing, but this explanation is hard to understand. Such a crossing is not known in ^{118}Xe up to date at this excitation energy and spin. A band crossing that was identified from the level scheme appears

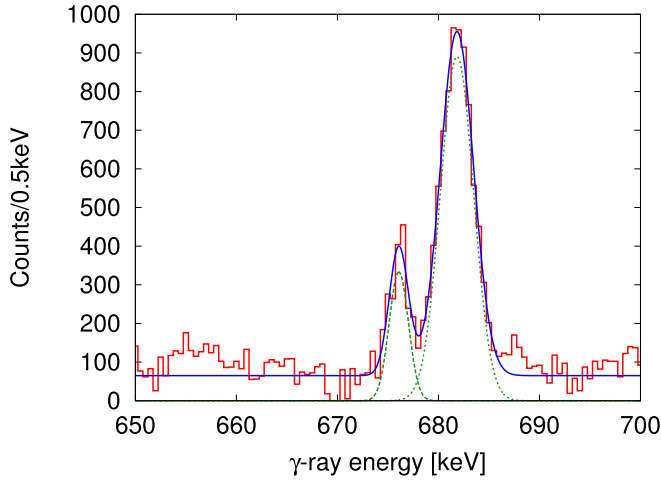


FIG. 4. Portion of the spectrum showing the $8^+ \rightarrow 6^+$ transition at forward angles with a gate on the shifted part of the feeding transition ($10^+ \rightarrow 8^+$). The histogram (red) show the experimental data together with a fit function of two gaussian functions (blue/solid), as well as their decomposition (green/dashed). No significant Doppler-shift attenuation effect is seen between the two components. See text for details.

close to the 10^+ state, similar to the heavier xenon isotopes. If delayed unobserved feeding is underestimated in a γ -ray singles experiment it leads to longer extracted level lifetimes and thus smaller $B(E2)$ values which would explain the small $B(E2; 6^+ \rightarrow 4^+)$ and $B(E2; 8^+ \rightarrow 6^+)$ values of Refs. [5–7].

The level scheme shows a γ -soft pattern similar to heavier nuclei in this mass region. This seems to warrant a discussion guided by the interacting boson model (IBM), which is presented hereafter. In terms of the IBM a transition from O(6) (γ -soft rotor) to U(5) (spherical vibrator) is expected for ^{118}Xe from the $N_\pi N_\nu$ scheme and comparisons to neighboring nuclei. In Fig. 5 the spin-dependent evolution of the transition strengths in the ground-state band (g.s.b.) of ^{118}Xe is presented. The trends for the IBM limits O(6), U(5), and SU(3) (axial-symmetric rotor) and an IBM calculation with fitted parameters are shown as well. The calculation has been carried out using the IBM1 [10] within the extended consistent Q -formalism (ECQF) [44] adding terms to the minimal ECQF Hamiltonian for compression of the τ multiplets and staggering in the quasi- γ band. The chosen Hamiltonian was

$$\begin{aligned} \hat{H} &= c \left[(1 - \zeta) \hat{n}_d - \frac{\zeta}{4N_B} \hat{Q}^\dagger \hat{Q}^\dagger + \lambda \hat{L} \hat{L} + \hat{C}_2(O(5)) \right] \\ \hat{C}_2(O(5)) &= \frac{2}{5} \beta \hat{L} \hat{L} + 4\beta \hat{T}^{(3)} \hat{T}^{(3)} \\ \hat{n}_d &= d^\dagger \cdot \tilde{d}, \quad \hat{Q}^\dagger = [s^\dagger \tilde{d} + d^\dagger s]^{(2)} + \chi [d^\dagger \tilde{d}]^{(2)}, \\ \hat{L} &= \sqrt{10} [d^\dagger \tilde{d}]^{(1)}, \quad \hat{T}^{(3)} = [d^\dagger \tilde{d}]^{(3)} \end{aligned} \quad (2)$$

with $N_B = 9$ the boson number, \hat{n}_d the d -boson number operator, \hat{Q}^\dagger the quadrupole operator, s^\dagger , s , d^\dagger , \tilde{d} the creation and annihilation operators for s and d bosons, $c = 1.126$ MeV a scaling parameter for the energies and ζ , χ the fitting parameters which span the space of the Hamiltonian, also

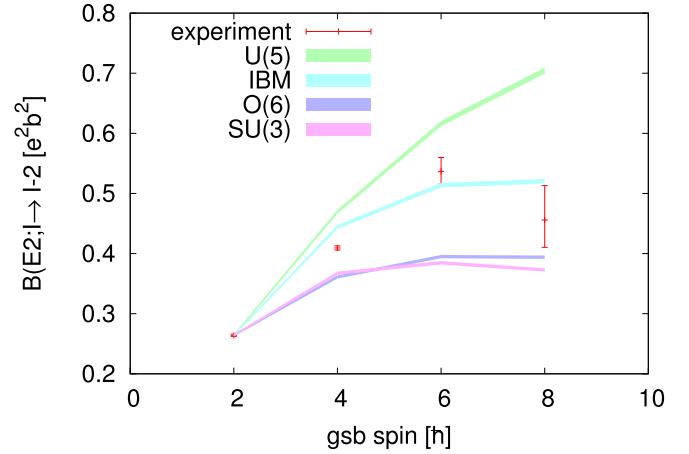


FIG. 5. Evolution of the transition strengths in the yrast band with respect to the initial spin. The experimental values, the trend for the three IBM limits and the result of an IBM1 calculation are shown. The ordering of the theoretical calculations in the legend reflects the predictions for transition strengths at the higher spins. See text for details.

known as the Casten triangle [45]. $\hat{T}(E2) = e_B \hat{Q}^\dagger$ is the $E2$ transition operator with $e_B = 0.129$ eb the effective boson charge. The experimental excitation energies are compared to the corresponding levels of the IBM calculation with $\zeta = 0.51$ and $\chi = -0.69$ ($\lambda = 0.009$, $\beta = -0.040$) in Fig. 6. $B(E2)$ values in the yrast band are given in the same figure, relative transition strengths in the quasi- γ band were calculated from the known branching ratios of Ref. [41] and are compared to the IBM calculation in Table II. The parameter ζ is close to the first-order phase transition between spherical and deformed shapes ($\zeta_c = \frac{16N_B}{34N_B - 27} = 0.516$ for $N_B = 9$). The overall agreement between the calculation and the experimental data is quite good, especially the spin-dependent evolution of collectivity for the yrast states corroborates the classification as a transitional nucleus.

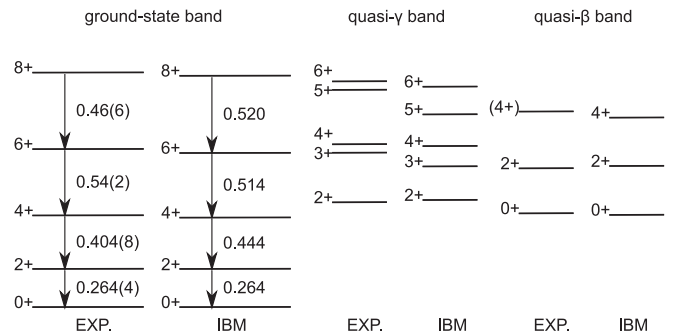


FIG. 6. Low-lying levels and $B(E2)$ values of the ground-state, the quasi- β and the quasi- γ band of ^{118}Xe . The experimentally known data for each band are displayed left to the results of the IBM1 calculation, using the ECQF Hamiltonian in Eq. (2). The number next to the arrow is the $B(E2)$ value for the corresponding transition in e^2b^2 . The parameters for this calculation are $\zeta = 0.51$, $\chi = -0.69$, $\lambda = 0.009$, $\beta = -0.040$, $c = 1.126$ MeV, and $e_b = 0.129$ eb.

TABLE II. Relative $B(E2)$ values of the quasi- γ band in ^{118}Xe calculated from known γ -ray energies and branching ratios of Ref. [41] and the IBM calculation. Since no mixing ratios are known, pure $E2$ transitions are assumed for all cases.

I_i^π	I_f^π	E_γ [keV]	$B(E2)$ Exp.	$B(E2)$ IBM
$2^+_\gamma \rightarrow$	2^+_{g}	590.6	36(12)	4
	0^+_{g}	928.1	1	1
$3^+_\gamma \rightarrow$	2^+_γ	438.0	49(13)	11
	2^+_{g}	1028.8	1	1
$4^+_\gamma \rightarrow$	2^+_γ	512.4	2.4(5)	3.8
	4^+_{g}	630.3	1	1
$5^+_\gamma \rightarrow$	3^+_γ	555.9	27(9)	10
	4^+_{g}	1112.1	1	1
$6^+_\gamma \rightarrow$	4^+_γ	555.8	4.6(10)	12.5
	6^+_{g}	599.8	1	1

The question raised in the introduction was if the unexpected behavior of transition strengths in even-even Sn and Te nuclei can be seen in the chain of the xenon isotopes. In Fig. 7 the evolution of $B(E2; 2^+ \rightarrow 0^+)$ and $B(E2; 4^+ \rightarrow 2^+)$ values for the even xenon isotopes between the shell closures at $N = 50$ and $N = 82$ is shown (cf. Fig. 1). At first glance no dip can be seen in the $B(E2; 2^+ \rightarrow 0^+)$ values around ^{120}Xe at midshell. The $B(E2)$ values from Ref. [55] are in this case most reliable, because other references (not shown) included feeding assumptions in their analyzes as pointed out in Ref. [56]. Within the error bars a linear slope between neutron midshell and the $N = 82$ shell closure is unambiguously present and follows the predictions of the $N_\pi N_\nu$ scheme. Therefore the reduction of $B(E2; 2^+ \rightarrow 0^+)$ values at midshell seems to disappear in the xenon isotopes. The data on the proton-rich side is too scarce to draw a clear conclusion. The

few data points below $N = 64$ hint for a symmetric slope with respect to midshell. So also the second hump of $B(E2; 2^+ \rightarrow 0^+)$ values that is noticeable in Sn isotopes around $N = 60$ turns out to vanish in the xenon isotopes. Nevertheless the $B_{4/2}$ ratio appears to be around unity for ^{114}Xe while for ^{116}Xe and heavier isotopes it remains at ratios expected from collective models. The drop of the $B(E2; 4^+ \rightarrow 2^+)$ value would be accordingly shifted from $N = 64$ in Sn to $N = 60$ in Xe (cf. Figs. 1, 7). In the tellurium isotopes the important data point at ^{116}Te is missing and one can only state that the critical point is either at $N = 62$ or $N = 64$. Unfortunately the transitions from the 2^+ and 4^+ states in ^{116}Te form a doublet and there exists even contradictory information about the sequence of γ rays, which makes an analysis very difficult. From the data in this work the idea that the reduction of $B(E2)$ values would be shifted to higher spins can be clearly ruled out. The lifetimes of the yrast 6^+ and 8^+ states have been corrected to lower values and the trend of transition strengths shows normal collective behavior. No unobserved band crossing at the 6^+ state is needed anymore to explain the spin-dependent evolution. Especially a low $B_{4/2}$ ratio as in the isotone ^{114}Sn is out of the question.

V. SUMMARY AND CONCLUSIONS

A RDDS experiment on ^{118}Xe has been conducted using a fusion-evaporation reaction. The data have been analyzed employing the DDCM using $\gamma\gamma$ coincidences and thus avoiding issues with a possible delayed sidefeeding of the levels of interest. The lifetimes of the 2^+ and 4^+ states are consistent with the most recent publication [5], but the new results have smaller uncertainties. The lifetimes of the 6^+ and 8^+ states are significantly shorter than the previous values removing the postulate of a band crossing close to the 6^+ state that was needed before to explain the spin-dependent trend of

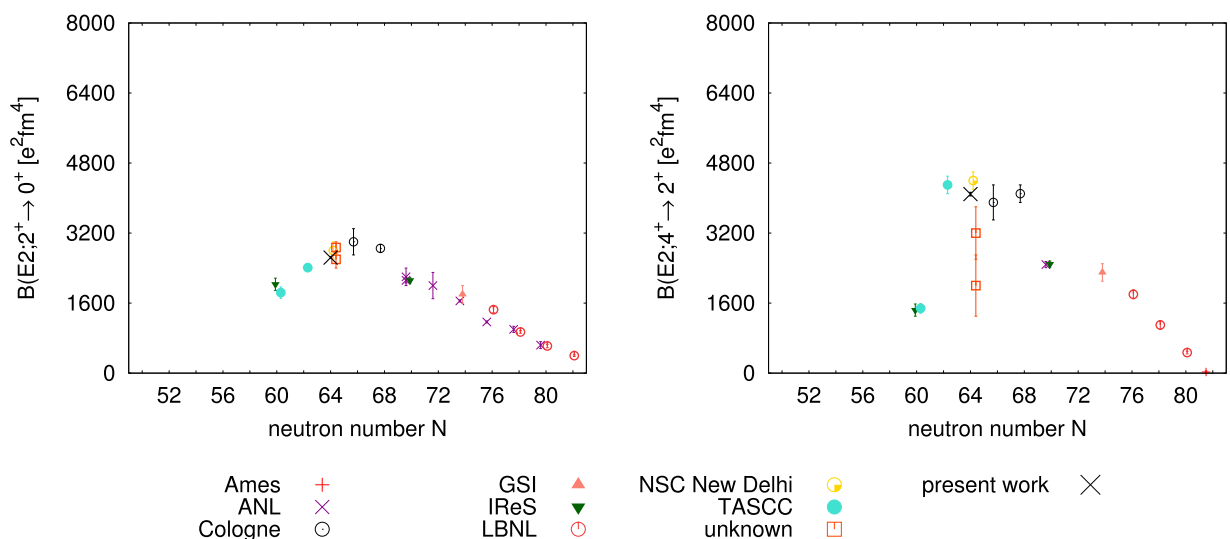


FIG. 7. Evolution of $B(E2; 2^+ \rightarrow 0^+)$ and $B(E2; 4^+ \rightarrow 2^+)$ values for the even xenon isotopes between the shell closures at $N = 50$ and $N = 82$. Different records for the same neutron number have been shifted slightly horizontally to sustain readability. The legend for both panels is given below, symbols are assigned to the facilities where the data was recorded. Compare Fig. 1 for the corresponding data on tin and tellurium isotopes. Experimental data taken from [5–7,46–55]. See text for details.

transition strengths. An IBM1 calculation has been performed classifying ^{118}Xe a transitional nucleus between spherical and deformed shapes. The sets of experimental data on Sn, Te, and Xe isotopes have been compared. Unlike in the $B(E2; 2^+ \rightarrow 0^+)$ systematics of the even-mass tin and tellurium isotopes, no dip at $N \approx 66$ and no second hump is seen in the corresponding data set for the most proton-rich xenon nuclei. The $B_{4/2}$ ratio in ^{114}Sn drops to unity staying low for lighter even Sn isotopes. The same effect is known for ^{114}Te while the data for the isotone ($N = 64$) ^{116}Te is missing. The same isotone ^{118}Xe discussed here shows a clearly collective behavior with a $B_{4/2}$ ratio of 1.55. The drop to unity is not seen before ^{114}Xe , which is also the lightest isotope with known transition strengths. It has to be mentioned that the transition strengths in ^{114}Xe have been measured employing the DDCM and $\gamma\gamma$ coincidences in Ref. [47], whereas the published $B(E2)$ values

in ^{116}Xe stem from a γ -ray singles experiment [46]. The low $B_{4/2}$ ratios cannot be explained with collective models. An interesting result is the shift of the critical point with drastically lowered $B(E2; 4^+ \rightarrow 2^+)$ strength. It seems to be displaced by two neutrons to lighter isotopes when adding two protons, instead of a direct connection to the $N = 64$ subshell closure. This hypothesis should be tested not only by experimental data on the most proton-rich nuclei in this mass region, but also with measurements of ^{116}Te and perhaps ^{116}Xe .

ACKNOWLEDGMENTS

This work was supported by the Deutsche Forschungsgemeinschaft (DFG) under Contract No. FR 3276/2-1 and by the U.S. Department of Energy, Office of Science, Office of Nuclear Physics, under Contract No. DE-AC02-06CH11357.

-
- [1] R. Casten, *Nucl. Phys. A* **443**, 1 (1985).
- [2] R. B. Cakirli, R. F. Casten, J. Jolie, and N. Warr, *Phys. Rev. C* **70**, 047302 (2004).
- [3] T. Togashi, Y. Tsunoda, T. Otsuka, N. Shimizu, and M. Honma, *Phys. Rev. Lett.* **121**, 062501 (2018).
- [4] M. Siciliano, J. Valiente-Dobón, A. Goasduff, F. Nowacki, A. Zuker, D. Bazzacco, A. Lopez-Martens, E. Clément, G. Benzoni, T. Braunroth, F. Crespi, N. Cieplicka-Oryńczak, M. Doncel, S. Ertürk, G. de France, C. Fransen, A. Gadea, G. Georgiev, A. Goldkuhle, U. Jakobsson, G. Jaworski, P. John, I. Kuti, A. Lemasson, T. Marchi, D. Mengoni, C. Michelagnoli, T. Mijatović, C. Müller-Gatermann, D. Napoli, J. Nyberg, M. Palacz, R. Pérez-Vidal, B. Saygi, D. Sohler, S. Szilner, D. Testov, M. Zielińska, D. Barrientos, B. Birkenbach, H. Boston, A. Boston, B. Cederwall, J. Collado, D. Cullen, P. Désesquelles, C. Domingo-Pardo, J. Dudouet, J. Eberth, F. Egea-Canet, V. González, L. Harkness-Brennan, H. Hess, D. Judson, A. Jungclaus, W. Kortem, M. Labiche, A. Lefevre, S. Leoni, H. Li, A. Maj, R. Menegazzo, B. Million, A. Pullia, F. Recchia, P. Reiter, M. Salsac, E. Sanchis, O. Stezowski, and C. Theisen, *Phys. Lett. B* **806**, 135474 (2020).
- [5] I. M. Govil, A. Kumar, H. Iyer, P. Joshi, S. K. Chamoli, R. Kumar, R. P. Singh, and U. Garg, *Phys. Rev. C* **66**, 064318 (2002).
- [6] T. Katou, Y. Tendow, H. Kumagai, Y. Gono, and A. Hashizume, *Proceedings of the International Conference on Nuclear Physics* (Nuclear Science Division, Lawrence Berkeley Laboratory, University of California, Berkeley, 1980).
- [7] A. M. Bergdolt, J. Chevallier, J. C. Merdinger, E. Bozek, and Z. Stachura, *Proceedings of the International Conference on Nuclear Structure* (Int. Academic Printing Co., Ltd. Japan, Tokyo, 1977).
- [8] A. Dewald, S. Harissopulos, and P. von Brentano, *Z. Phys. A* **334**, 163 (1989).
- [9] N.-G. Jonsson, A. Bäcklin, J. Kantele, R. Julin, M. Luontama, and A. Passoja, *Nucl. Phys. A* **371**, 333 (1981).
- [10] A. Arima and F. Iachello, *Phys. Rev. Lett.* **35**, 1069 (1975).
- [11] G. Guastalla, D. D. DiJulio, M. Górska, J. Cederkäll, P. Boutachkov, P. Golubev, S. Pietri, H. Grawe, F. Nowacki, K. Sieja, A. Algora, F. Ameil, T. Arici, A. Atac, M. A. Bentley, A. Blazhev, D. Bloor, S. Brambilla, N. Braun, F. Camera, Z. Dombrádi, C. Domingo Pardo, A. Estrade, F. Farinon, J. Gerl, N. Goel, J. Grębosz, T. Habermann, R. Hoischen, K. Jansson, J. Jolie, A. Jungclaus, I. Kojouharov, R. Knoebel, R. Kumar, J. Kurcewicz, N. Kurz, N. Lalović, E. Merchan, K. Moschner, F. Naqvi, B. S. Nara Singh, J. Nyberg, C. Nociforo, A. Obertelli, M. Pfützner, N. Pietralla, Z. Podolyák, A. Prochazka, D. Ralet, P. Reiter, D. Rudolph, H. Schaffner, F. Schirru, L. Scruton, D. Sohler, T. Swaleh, J. Taprogge, Z. Vajta, R. Wadsworth, N. Warr, H. Weick, A. Wendt, O. Wieland, J. S. Winfield, and H. J. Wollersheim, *Phys. Rev. Lett.* **110**, 172501 (2013).
- [12] V. M. Bader, A. Gade, D. Weisshaar, B. A. Brown, T. Baugher, D. Bazin, J. S. Berryman, A. Ekström, M. Hjorth-Jensen, S. R. Stroberg, W. B. Walters, K. Wimmer, and R. Winkler, *Phys. Rev. C* **88**, 051301(R) (2013).
- [13] P. Doornenbal, S. Takeuchi, N. Aoi, M. Matsushita, A. Obertelli, D. Steppenbeck, H. Wang, L. Audirac, H. Baba, P. Bednarczyk, S. Boissinot, M. Ciemala, A. Corsi, T. Furumoto, T. Isobe, A. Jungclaus, V. Lapoux, J. Lee, K. Matsui, T. Motobayashi, D. Nishimura, S. Ota, E. C. Pollacco, H. Sakurai, C. Santamaria, Y. Shiga, D. Sohler, and R. Taniuchi, *Phys. Rev. C* **90**, 061302(R) (2014).
- [14] C. Vaman, C. Andreoiu, D. Bazin, A. Becerril, B. A. Brown, C. M. Campbell, A. Chester, J. M. Cook, D. C. Dinca, A. Gade, D. Galaviz, T. Glasmacher, M. Hjorth-Jensen, M. Horoi, D. Miller, V. Moeller, W. F. Mueller, A. Schiller, K. Starosta, A. Stolz, J. R. Terry, A. Volya, V. Zelevinsky, and H. Zwahlen, *Phys. Rev. Lett.* **99**, 162501 (2007).
- [15] A. Ekström, J. Cederkäll, C. Fahlander, M. Hjorth-Jensen, F. Ames, P. A. Butler, T. Davinson, J. Eberth, F. Fincke, A. Görge, M. Górska, D. Habs, A. M. Hurst, M. Huyse, O. Ivanov, J. Iwanicki, O. Kester, U. Köster, B. A. Marsh, J. Mierzejewski, P. Reiter, H. Scheit, D. Schwalm, S. Siem, G. Sletten, I. Stefanescu, G. M. Tveten, J. Van de Walle, P. Van Duppen, D. Voulot, N. Warr, D. Weisshaar, F. Wenander, and M. Zielińska, *Phys. Rev. Lett.* **101**, 012502 (2008).
- [16] A. Banu, J. Gerl, C. Fahlander, M. Górska, H. Grawe, T. R. Saito, H.-J. Wollersheim, E. Caurier, T. Engeland, A. Gniady, M. Hjorth-Jensen, F. Nowacki, T. Beck, F. Becker, P. Bednarczyk, M. A. Bentley, A. Bürger, F. Cristancho, G. d. Angelis, Z. Dombrádi, P. Doornenbal, H. Geissel, J. Grebosz, G. Hammond, M. Hellström, J. Jolie, I. Kojouharov, N. Kurz,

- R. Lozeva, S. Mandal, N. Märginean, S. Muralithar, J. Nyberg, J. Pochodzalla, W. Prokopowicz, P. Reiter, D. Rudolph, C. Rusu, N. Saito, H. Schaffner, D. Sohler, H. Weick, C. Wheldon, and M. Winkler, *Phys. Rev. C* **72**, 061305(R) (2005).
- [17] J. Cederkäll, A. Ekström, C. Fahlander, A. M. Hurst, M. Hjorth-Jensen, F. Ames, A. Banu, P. A. Butler, T. Davinson, U. Datta Pramanik, J. Eberth, S. Franchoo, G. Georgiev, M. Górska, D. Habs, M. Huyse, O. Ivanov, J. Iwanicki, O. Kester, U. Köster, B. A. Marsh, O. Niedermaier, T. Nilsson, P. Reiter, H. Scheit, D. Schwalm, T. Sieber, G. Sletten, I. Stefanescu, J. Van de Walle, P. Van Duppen, N. Warr, D. Weisshaar, and F. Wenander, *Phys. Rev. Lett.* **98**, 172501 (2007).
- [18] G. J. Kumbartzki, N. Benczer-Koller, K.-H. Speidel, D. A. Torres, J. M. Allmond, P. Fallon, I. Abramovic, L. A. Bernstein, J. E. Bevins, H. L. Crawford, Z. E. Guevara, G. Gürdal, A. M. Hurst, L. Kirsch, T. A. Laplace, A. Lo, E. F. Matthews, I. Mayers, L. W. Phair, F. Ramirez, S. J. Q. Robinson, Y. Y. Sharon, and A. Wiens, *Phys. Rev. C* **93**, 044316 (2016).
- [19] A. Jungclaus, J. Walker, J. Leske, K.-H. Speidel, A. Stuchbery, M. East, P. Boutachkov, J. Cederkäll, P. Doornenbal, J. Egido, A. Ekström, J. Gerl, R. Gernhäuser, N. Goel, M. Górska, I. Kojouharov, P. Maier-Komor, V. Modamio, F. Naqvi, N. Pietralla, S. Pietri, W. Prokopowicz, H. Schaffner, R. Schwengner, and H.-J. Wollersheim, *Phys. Lett. B* **695**, 110 (2011).
- [20] R. Kumar, M. Saxena, P. Doornenbal, A. Jhingan, A. Banerjee, R. K. Bhowmik, S. Dutt, R. Garg, C. Joshi, V. Mishra, P. J. Napiorkowski, S. Prajapati, P.-A. Söderström, N. Kumar, and H.-J. Wollersheim, *Phys. Rev. C* **96**, 054318 (2017).
- [21] J. M. Allmond, A. E. Stuchbery, A. Galindo-Uribarri, E. Padilla-Rodal, D. C. Radford, J. C. Batchelder, C. R. Bingham, M. E. Howard, J. F. Liang, B. Manning, S. D. Pain, N. J. Stone, R. L. Varner, and C.-H. Yu, *Phys. Rev. C* **92**, 041303(R) (2015).
- [22] M. Spieker, P. Petkov, E. Litvinova, C. Müller-Gatermann, S. G. Pickstone, S. Prill, P. Scholz, and A. Zilges, *Phys. Rev. C* **97**, 054319 (2018).
- [23] J. Gableske, A. Dewald, H. Tiesler, M. Wilhelm, T. Klemme, O. Vogel, I. Schneider, R. Peusquens, S. Kasemann, K. Zell, P. von Brentano, P. Petkov, D. Bazzacco, C. R. Alvarez, S. Lunardi, G. de Angelis, M. de Poli, and C. Fahlander, *Nucl. Phys. A* **691**, 551 (2001).
- [24] P. Doornenbal, P. Reiter, H. Grawe, H. J. Wollersheim, P. Bednarczyk, L. Caceres, J. Cederkäll, A. Ekström, J. Gerl, M. Górska, A. Jhingan, I. Kojouharov, R. Kumar, W. Prokopowicz, H. Schaffner, and R. P. Singh, *Phys. Rev. C* **78**, 031303(R) (2008).
- [25] G. J. Kumbartzki, N. Benczer-Koller, D. A. Torres, B. Manning, P. D. O'Malley, Y. Y. Sharon, L. Zamick, C. J. Gross, D. C. Radford, S. J. Q. Robinson, J. M. Allmond, A. E. Stuchbery, K.-H. Speidel, N. J. Stone, and C. R. Bingham, *Phys. Rev. C* **86**, 034319 (2012).
- [26] J. M. Allmond, D. C. Radford, C. Baktash, J. C. Batchelder, A. Galindo-Uribarri, C. J. Gross, P. A. Hausladen, K. Lagergren, Y. Larochele, E. Padilla-Rodal, and C.-H. Yu, *Phys. Rev. C* **84**, 061303(R) (2011).
- [27] D. Radford, C. Baktash, C. Barton, J. Batchelder, J. Beene, C. Bingham, M. Caprio, M. Danchev, B. Fuentes, A. Galindo-Uribarri, J. G. del Campo, C. Gross, M. Halbert, D. Hartley, P. Hausladen, J. Hwang, W. Krolas, Y. Larochele, J. Liang, P. Mueller, E. Padilla, J. Pavan, A. Piechaczek, D. Shapira, D. Stracener, R. Varner, A. Woehr, C.-H. Yu, and N. Zamfir, *Nucl. Phys. A* **752**, 264 (2005).
- [28] D. Rosiak, M. Seidlitz, P. Reiter, H. Naïdja, Y. Tsunoda, T. Togashi, F. Nowacki, T. Otsuka, G. Colò, K. Arnsward, T. Berry, A. Blazhev, M. J. G. Borge, J. Cederkäll, D. M. Cox, H. De Witte, L. P. Gaffney, C. Henrich, R. Hirsch, M. Huyse, A. Illana, K. Johnston, L. Kaya, T. Kröll, M. L. Lozano Benito, J. Ojala, J. Pakarinen, M. Queiser, G. Rainovski, J. A. Rodriguez, B. Siebeck, E. Siesling, J. Snäll, P. Van Duppen, A. Vogt, M. von Schmid, N. Warr, F. Wenander, and K. O. Zell (MINIBALL and HIE-ISOLDE Collaborations), *Phys. Rev. Lett.* **121**, 252501 (2018).
- [29] T. Bäck, C. Qi, F. Ghazi Moradi, B. Cederwall, A. Johnson, R. Liotta, R. Wyss, H. Al-Azri, D. Bloor, T. Brock, R. Wadsworth, T. Grahn, P. T. Greenlees, K. Hauschild, A. Herzan, U. Jacobsson, P. M. Jones, R. Julin, S. Juutinen, S. Ketelhut, M. Leino, A. Lopez-Martens, P. Nieminen, P. Peura, P. Rakhila, S. Rinta-Antila, P. Ruotsalainen, M. Sandzelius, J. Sarén, C. Scholey, J. Sorri, J. Uusitalo, S. Go, E. Ideguchi, D. M. Cullen, M. G. Procter, T. Braunroth, A. Dewald, C. Fransen, M. Hackstein, J. Litzinger, and W. Rother, *Phys. Rev. C* **84**, 041306(R) (2011).
- [30] M. Doncel, T. Bäck, D. M. Cullen, D. Hodge, C. Qi, B. Cederwall, M. J. Taylor, M. Procter, K. Auranen, T. Grahn, P. T. Greenlees, U. Jakobsson, R. Julin, S. Juutinen, A. Herzán, J. Konki, M. Leino, J. Pakarinen, J. Partanen, P. Peura, P. Rakhila, P. Ruotsalainen, M. Sandzelius, J. Sarén, C. Scholey, J. Sorri, S. Stolze, and J. Uusitalo, *Phys. Rev. C* **91**, 061304(R) (2015).
- [31] M. Doncel, T. Bäck, C. Qi, D. M. Cullen, D. Hodge, B. Cederwall, M. J. Taylor, M. Procter, M. Giles, K. Auranen, T. Grahn, P. T. Greenlees, U. Jakobsson, R. Julin, S. Juutinen, A. Herzán, J. Konki, J. Pakarinen, J. Partanen, P. Peura, P. Rakhila, P. Ruotsalainen, M. Sandzelius, J. Sarén, C. Scholey, J. Sorri, S. Stolze, and J. Uusitalo, *Phys. Rev. C* **96**, 051304(R) (2017).
- [32] O. Möller, N. Warr, J. Jolie, A. Dewald, A. Fitzler, A. Linnemann, K. O. Zell, P. E. Garrett, and S. W. Yates, *Phys. Rev. C* **71**, 064324 (2005).
- [33] A. Pasternak, J. Srebrny, A. Efimov, V. Mikhajlov, E. Podsvirova, C. Droste, T. Morek, S. Juutinen, G. Hagemann, M. Piiparinen, S. Törmänen, and A. Virtanen, *Eur. Phys. J. A* **13**, 435 (2002).
- [34] M. Saxena, R. Kumar, A. Jhingan, S. Mandal, A. Stolarz, A. Banerjee, R. K. Bhowmik, S. Dutt, J. Kaur, V. Kumar, M. Modou Mbaye, V. R. Sharma, and H.-J. Wollersheim, *Phys. Rev. C* **90**, 024316 (2014).
- [35] A. Kleinfeld, G. Mäggi, and D. Werdecker, *Nucl. Phys. A* **248**, 342 (1975).
- [36] A. Bockisch and A. Kleinfeld, *Nucl. Phys. A* **261**, 498 (1976).
- [37] A. E. Stuchbery, J. M. Allmond, A. Galindo-Uribarri, E. Padilla-Rodal, D. C. Radford, N. J. Stone, J. C. Batchelder, J. R. Beene, N. Benczer-Koller, C. R. Bingham, M. E. Howard, G. J. Kumbartzki, J. F. Liang, B. Manning, D. W. Stracener, and C.-H. Yu, *Phys. Rev. C* **88**, 051304(R) (2013).
- [38] C. Barton, M. Caprio, D. Shapira, N. Zamfir, D. Brenner, R. Gill, T. Lewis, J. Cooper, R. Casten, C. Beausang, R. Krücken, and J. Novak, *Phys. Lett. B* **551**, 269 (2003).
- [39] M. Danchev, G. Rainovski, N. Pietralla, A. Gargano, A. Covello, C. Baktash, J. R. Beene, C. R. Bingham, A. Galindo-Uribarri, K. A. Gladnishi, C. J. Gross, V. Y. Ponomarev, D. C. Radford, L. L. Riedinger, M. Scheck, A. E. Stuchbery,

- J. Wambach, C.-H. Yu, and N. V. Zamfir, *Phys. Rev. C* **84**, 061306(R) (2011).
- [40] A. Dewald, O. Möller, and P. Petkov, *Prog. Part. Nucl. Phys.* **67**, 786 (2012).
- [41] J. M. Sears, D. B. Fossan, G. R. Gluckman, J. F. Smith, I. Thorslund, E. S. Paul, I. M. Hibbert, and R. Wadsworth, *Phys. Rev. C* **57**, 2991 (1998).
- [42] B. Saha, Bestimmung der Lebensdauern kollektiver Kernanregungen in ^{124}Xe und Entwicklung von entsprechender Analysesoftware, Ph.D. thesis, Universität zu Köln, 2004.
- [43] P. Petkov, D. Tonev, J. Gableske, A. Dewald, T. Klemme, and P. von Brentano, *Nucl. Instrum. Methods Phys. Res. A* **431**, 208 (1999).
- [44] D. D. Warner and R. F. Casten, *Phys. Rev. C* **28**, 1798 (1983).
- [45] J. Jolie, R. F. Casten, P. von Brentano, and V. Werner, *Phys. Rev. Lett.* **87**, 162501 (2001).
- [46] J. DeGraaf, M. Cromaz, T. E. Drake, V. P. Janzen, D. C. Radford, and D. Ward, *Phys. Rev. C* **58**, 164 (1998).
- [47] G. de Angelis, A. Gadea, E. Farnea, R. Isocrate, P. Petkov, N. Marginean, D. Napoli, A. Dewald, M. Bellato, A. Bracco, F. Camera, D. Curien, M. De Poli, E. Fioretto, A. Fitzler, S. Kasemann, N. Kintz, T. Klug, S. Lenzi, S. Lunardi, R. Menegazzo, P. Pavan, J. Pedroza, V. Pucknell, C. Ring, J. Sampson, and R. Wyss, *Phys. Lett. B* **535**, 93 (2002).
- [48] P. Petkov, R. Krücken, A. Dewald, P. Sala, G. Böhm, J. Altmann, A. Gelberg, P. von Brentano, R. Jolos, and W. Andrejtscheff, *Nucl. Phys. A* **568**, 572 (1994).
- [49] W. F. Mueller, M. P. Carpenter, J. A. Church, D. C. Dinca, A. Gade, T. Glasmacher, D. T. Henderson, Z. Hu, R. V. F. Janssens, A. F. Lisetskiy, C. J. Lister, E. F. Moore, T. O. Pennington, B. C. Perry, I. Wiedenhöver, K. L. Yurkewicz, V. G. Zelevinsky, and H. Zwahlen, *Phys. Rev. C* **73**, 014316 (2006).
- [50] B. Saha, A. Dewald, O. Möller, R. Peusquens, K. Jessen, A. Fitzler, T. Klug, D. Tonev, P. von Brentano, J. Jolie, B. J. P. Gall, and P. Petkov, *Phys. Rev. C* **70**, 034313 (2004).
- [51] G. Rainovski, N. Pietralla, T. Ahn, L. Coquard, C. Lister, R. Janssens, M. Carpenter, S. Zhu, L. Bettermann, J. Jolie, W. Rother, R. Jolos, and V. Werner, *Phys. Lett. B* **683**, 11 (2010).
- [52] J. Srebny, T. Czosnyka, W. Karczmarczyk, P. Napiorkowski, C. Droste, H.-J. Wollersheim, H. Emling, H. Grein, R. Kulessa, D. Cline, and C. Fahlander, *Nucl. Phys. A* **557**, 663 (1993).
- [53] G. Jakob, N. Benczer-Koller, G. Kumbartzki, J. Holden, T. J. Mertzimekis, K.-H. Speidel, R. Ernst, A. E. Stuchbery, A. Pakou, P. Maier-Komor, A. Macchiavelli, M. McMahan, L. Phair, and I. Y. Lee, *Phys. Rev. C* **65**, 024316 (2002).
- [54] J. A. Morman, W. C. Schick, and W. L. Talbert, *Phys. Rev. C* **11**, 913 (1975).
- [55] A. Dewald, P. Petkov, R. Wrzal, G. Siems, R. Wirowski, P. Sala, G. Böhm, A. Gelberg, K. Zell, P. von Brentano, P. Nolan, A. Kirwan, D. Bishop, R. Julin, A. Lampinen, and J. Hattula, *Proceedings of the XXV Zakopane School on Physics* (World Scientific, 1990).
- [56] J. C. Walpe, B. F. Davis, S. Naguleswaran, W. Reviol, U. Garg, X.-W. Pan, D. H. Feng, and J. X. Saladin, *Phys. Rev. C* **52**, 1792 (1995).